
Article:
Zhang, L. and Lang, Z. (2018) Wavelet Energy Transmissibility Function and its Application to Wind Turbine Bearing Condition Monitoring. IEEE Transactions on Sustainable Energy, 9 (4). pp. 1833-1843. ISSN: 1949-3029

https://doi.org/10.1109/TSTE.2018.2816738

Wavelet Energy Transmissibility Function and its Application to Wind Turbine Bearing Condition Monitoring

Long Zhang, *Member, IEEE,* Zi-Qiang Lang

***Abstract*—Condition or health monitoring techniques and methods have been widely used for engineering systems fault detection and diagnosis. However, there is a major challenge with monitoring the systems operating under time varying loadings especially when the system loads are unknown or hard to measure. To address this problem, a new concept, wavelet energy transmissibility function (WETF), is proposed in this paper. The main advantage of this new method is that it can remove the impact of varying loadings but it does not require any loading information. Further the proposed method is robust to noise and is sensitive to system property changes. The effectiveness of the proposed method has been well demonstrated by a numerical example, the theoretical study and the analysis of the field vibration data from bearings of operating wind turbines.**

***Index Terms*—Wavelet energy transmissibility functions (WETF), Wind turbine, Condition monitoring,**

I. Introduction

Frequency domain methods have been widely used for the condition monitoring of engineering systems. The fundamental principal is that damaged systems can produce frequency characteristics that is different from those under normal conditions. For example, some faults can cause frequency shocks, spikes or sidebands. If the monitored systems are under steady or stationary operating conditions, Fast Fourier Transform (FFT), modulation sidebands, envelope analysis, cepstrum analysis, skewness and kurtosis have been successfully used in many applications [1], [2], [3]. However, if the monitored systems are under non-stationary operating conditions, such as in the case of wind turbines, the frequency information may vary with the system dynamic loadings, which is referred to as the variable loading problems [4], [5], [6], [7], [8], [9], [10]. Variable loadings can result in difficulties in using traditional frequency domain techniques. To address the dynamic loading problems, time-frequency methods, such as short-time FFT, Empirical model decomposition, Hilbert transform, and wavelet transform and their modifications, can be used in many cases including both online and realtime and offline applications [11], [12], [13], [14], [15], [16]. These methods are also well studied and used in other fields, such as structure health monitoring [17], [18].

Alternatively, the frequency response function (FRF) is a promising technique to remove the dynamic loading effects. FRF is defined as the spectra ratio between the dynamic response and corresponding loading input [19], [20], [21]. Due to the ratio operation, the effect of the input loading can often be eliminated, producing FRF solely dependent on system physical properties. For the purpose of health monitoring, the estimated FRFs can be compared with their baseline values [19], [22]. If the changes are beyond a warning threshold, the inspected system or component may have some physical damage. According to the definition of FRF, the computation of the FRF needs to measure the system input and response simultaneously. However, the information of input loading is often not available. In the case, FRF can not be used for condition monitoring purpose.

As a similar concept to FRF, transmissibility function (TF) is defined as the ratio of two different FRFs and is also equal to the ratio of the spectra of two different responses. In other words, unlike FRF which requires both system input and outputs, TF only requires system outputs or measured responses. TF can be used to represent the system physical properties. For example, for a multi-degree of freedom (MDOF) system, TF is solely dependent on modal parameters including mass, stiffness and damping [23], [24], [25], [22]. TF based condition monitoring has been widely used in many applications [24], [26], [27], [28], [28], [21]. A good review on the transmissibility analysis can be found in [27].

In practical applications, FRF and TF are often estimated from measured data using Fourier transform [29]. Most recently, instead of Fourier transform, the wavelet transform is proposed to compute FRF [30] and experimental investigations on wavelet based FRF with validations to detect abrupt change in stiffness were carried out in [31]. The new wavelet FRF is the ratio of coefficients of wavelet transforms of system input and output. A similar type of concept employing the ratios of wavelet coefficients at different frequency bands were proposed in [32] to identify time-varying and nonlinear systems. Due to the relationship between FRF and TF, wavelet FRF can be naturally extended to wavelet TF (WTF) as the ratio between wavelet coefficients of two different system responses. However, it is found in the present study that it is often difficult to produce an consistent WTF using real data. The main reason for this can be due to the variable or dynamic loading effect as the estimated WTF may have different values under different loading conditions. Another reason can be due to the noise effect which can easily corrupt useful information in data, especially data with small amplitudes.

In the present study, a new concept, wavelet energy trans-

L. Zhang is with the School of Electrical and Electronic Engineering, Univerity of Manchester, UK, M13 9PL, e-mail: long.zhang@manchester.ac.uk and Z. Lang is with the Department of Automatic Control of System Engineering, The University of Sheffield, Sheffield, UK, S1 3JD, e-mail: z.lang@sheffield.ac.uk

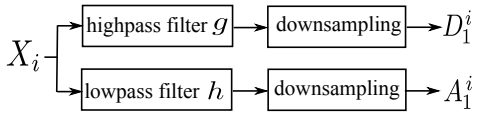

Fig. 1. wavelet level 1 decomposition

missibility function (WETF), is proposed to overcome the effects of dynamic loadings and noise on the data analysis. The proposed method is evaluated using a large amount of field data from operating wind turbine bearings and promising results are achieved.

II. Wavelet Transmissibility Function (WTF)

When system responses are measured by multiple sensors simultaneously, the wavelet transmissibility can be calculated using the ratio of coefficients resulting from wavelet transforms of two different measurements. Therefore, the wavelet coefficients need to be first obtained. Suppose there are n measurements which are denoted as $[X_1, ..., X_i, ..., X_n]$ where $X_i = [x_i(1), ..., x_i(N)]^T$ with N being the data length. The wavelet transform of $X_i, i = 1, ..., n$, is given by

$$W_i(a,b) = a^{-\frac{1}{2}} \int x_i(t)\varphi(\frac{t-b}{a})dt \tag{1}$$

where φ is a wavelet function and a, b are dilation and translation parameters, respectively. The integral operation is computationally expensive, therefore a direct method is not preferable in practice. To improve the computational efficiency, the multiple resolution analysis (MRA) method was proposed in [33], which makes wavelet analysis be widely used in all aspects of engineering and science fields due to its excellent computational efficiency. The MRA uses multiple levels decomposition to compute coarse-to-fine frequency resolutions. In each level of decomposition, MRA first involves computing the convolutions with high pass filter g and low pass filter h where the filters are determined by the wavelet orthonormal basis, and then adopts downsamplings for both filtered results. For level one decomposition, the original signal X_i is decomposed to a detailed part D_1^i and an approximation part A_1^i. More specifically, the decomposition process can be denoted as

$$D_1^i = (X_i * g) \downarrow 2 \tag{2}$$

$$A_1^i = (X_i * h) \downarrow 2 \tag{3}$$

where

$$X_i * g = \{\sum_k x_i(k)g(n-k), n = 1, ..., N\} \tag{4}$$

and

$$X_i * h = \{\sum_k x_i(k)h(n-k), n = 1, ..., N\} \tag{5}$$

and $\downarrow 2$ indicates the downsampling by 2. To make it clear, the level 1 decomposition is illustrated in Fig. 1. The approximation part A_1^i can be further decomposed using the same procedure. The second decomposition is called level 2 decomposition. The decomposition continues until a preset level is satisfied. For the wavelet transform with J level decomposition, it can be described in Fig. 2 and wavelet coefficients are given by

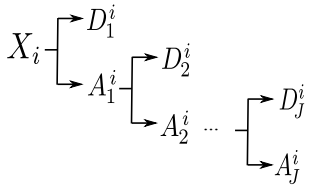

Fig. 2. J level wavelet decomposition

$$\begin{aligned} W_i &= \{A_J^i, D_J^i, D_{J-1}^i, \ldots, D_1^i\} \\ &= \{v_i(r), r = 1, \ldots, R\} \end{aligned} \tag{6}$$

The TF is the ratio between two different measurements. Let ith and jth denote the two different measurement indexes, where $i = 1, ..., n-1, j = i+1, ..., n$, and the transmissibility function between two measurements can be written as

$$T_{ij} = [t_{ij}(1), ..., t_{ij}(r), ..., t_{ij}(R)] \tag{7}$$

where

$$t_{ij}(r) = \frac{\nu_i(r)}{\nu_j(r)} \tag{8}$$

The total number of such transmissibility functions is $L = (n-1)n/2$. These functions will be denoted as

$$\begin{aligned} &\{t_{ij}(r), i = 1, ..., n-1, j = i+1, ..., n\} \\ =&\{\tau_l(r), l = 1, ..., L\} \end{aligned} \tag{9}$$

Therefore, the values of all the transmissibility functions can be written as

$$\Gamma = \begin{bmatrix} \tau_1(1) & \tau_1(2) & \ldots & \tau_1(R) \\ \tau_2(1) & \tau_2(2) & \ldots & \tau_2(R) \\ \vdots & \vdots & \vdots & \vdots \\ \tau_L(1) & \tau_L(2) & \ldots & \tau_L(R) \end{bmatrix} \tag{10}$$

For the purpose of damage detection, the transmissibility correlation (TC) between healthy ${}^h\tau(r)$ and in-service $\tau(r)$ can be used, which is defined as

$$TC(r) = \frac{|\sum_{l=1}^L \tau_l(r)^h\tau_l(r)|^2}{[\sum_{l=1}^L \tau_l(r)\tau_l(r)][\sum_{l=1}^L {}^h\tau_l(r)^h\tau_l(r)]} \tag{11}$$

Transmissibility damage indicator (TDI) is the average of transmissibility correlations over all the parameters $\{1, \ldots, R\}$ given by [34]

$$TDI = \frac{1}{R}\sum_{r=1}^R TC(r) \tag{12}$$

The wavelet TDI measures the similarities between normal condition and monitored condition. If the two conditions are similar, the correlation values at all frequencies are high. Otherwise, the correlation values are low. It is worth mentioning that the range of wavelet TDI values is between 0 and 1. If wavelet TDI value is 1 or near 1, it means the monitored condition is healthy. If it is smaller than 1 or near 0, it indicates damage may happen. In general, the more serious the damage is, the smaller the TDI value will be [21].

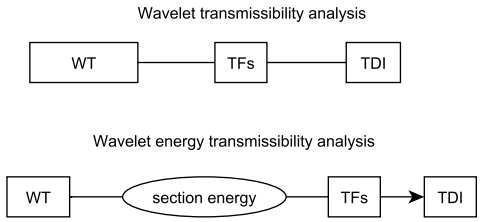

Fig. 3. wavelet section energy transmissibility procedure

III. Wavelet Energy Transmissibility Function (WETF)

In theory, the WTF should be unique under the same system condition. However, in practice, the WTF is determined from measured data and the results can therefore be affected by many issues. First, the WTF can be easily corrupted by the noise due to that a ratio calculation for estimating WTF is used. Further, under different loading conditions, the WTF often varies because of the loading effects. For example, a wind turbine operates under time-varying wind loads, and therefore it has time-varying system responses, say vibrations. As WTF is estimated using measured vibration data in practice, the estimated values may not be consistent under different wind loads. In other words, the effects of time-varying wind loads may not be fully eliminated. These two reasons may prevent the wide applications of WTF. In order to address these issues, in this section, a new concept, called as wavelet energy transmissibility function (WETF), is proposed. Unlike the WTF that is the ratio of the coefficients between wavelet transforms of two different responses [35], [36], the WETF is the ratio of wavelet energy between the wavelet transforms of two different responses. Fig. 3 illustrates the difference between WTF and WETF. Here, the wavelet energy is defined as the root mean squares (RMS) of a group of wavelet coefficients. Suppose the R wavelet coefficients are divided into Z groups and each group has m wavelet coefficients. More specifically, from the original wavelet coefficients in Equation (6), the new wavelet energy (WE) can be obtained as

$$WE_i = \{e_i(z), z = 1, ..., Z\} \tag{13}$$

where

$$\begin{bmatrix} e_i(1) = RMS(\nu_i(1), ..., \nu_i(m)) \\ e_i(2) = RMS(\nu_i(m+1), ..., \nu_i(2m)) \\ \vdots \\ e_i(Z) = RMS(\nu_i((Z-1)m+1), ..., \nu_i(Zm)) \end{bmatrix} \tag{14}$$

and

$$\begin{aligned} e_i(z) &= RMS(\nu_i((z-1)m+1), ..., \nu_i(zm)) \\ &= \sqrt{\frac{1}{m} \sum_{h=(z-1)m+1}^{zm} \nu_i^2(h)} \end{aligned} \tag{15}$$

and $zm = R$. Then the WETF is defined as

$$T_{ij} = [t_{ij}(1), ..., t_{ij}(z), ..., t_{ij}(Z)] \tag{16}$$

where

$$t_{ij}(z) = \frac{e_i(z)}{e_j(z)} \tag{17}$$

The total number of the WETF is also $L = (n-1)n/2$ and these functions will be represented as:

$$\begin{aligned} &\{t_{ij}(z), i = 1, ..., n-1, j = i+1, ..., n\} \\ =&\{\tau_l(z), l = 1, ..., L\} \end{aligned} \tag{18}$$

In this case, the transmissibility correlation (TC) is changed to

$$TC(z) = \frac{|\sum_{l=1}^{L} \tau_l(z)^h \tau_l(z)|^2}{[\sum_{l=1}^{L} \tau_l(z)\tau_l(z)][\sum_{l=1}^{L} {}^h\tau_l(z)^h\tau_l(z)]} \tag{19}$$

and TDI is the average of the TCs over all the Z groups given by

$$TDI = \frac{1}{Z} \sum_{z=1}^{Z} TC(z) \tag{20}$$

The ultimate objective of grouping wavelet coefficients is to make WTF less sensitive to variable loadings and noise. In each group, its RMS value is the wavelet energy indicator, which is a robust and stable indicator in condition monitoring, and can help reduce sensitivity to noise and dynamic loadings without sacrificing sensitivity to the changes in system properties. The grouping number m can be tuned to control the tradeoff between sensitivities and robustness.

To make the new concept clear and demonstrate its robustness to noise and time varying loading, a numerical example of a mass-damping-spring system is used to show its relationship with conventional TF and advantages over WTF. For the mass-damping-spring system, the TF is only dependent on the mass, damping and spring parameters. Here, suppose one TF that describes the relationship between two measurements in Laplace transform is given by [37]

$$TF(s) = \frac{36s + 400}{s^2 + 36s + 400} \tag{21}$$

where s represents the frequency operator in the Laplace domain. The plot of the frequency response function of the TF is shown in Fig. 4. The magnitude represents the frequency gain of the second measurement over the first measurement. It can be seen that the low frequency gains are around 1 and the high frequency gains fall rapidly. Moreover, suppose the first measurement contains a combination of sine waves over the frequency range from 0 Hz to 50 Hz, with the difference between two consecutive frequencies being 0.2 Hz and the second measurement is the response of the system represented by the TF to the first measurement. To produce the wavelet based TF, the wavelet function and the decomposition level have to be chosen first. Here, the low pass wavelet filter in (5) and high pass filter in (4) are chosen as h=[0,0,0,0,0.1768,0.5303,0.5303,0.1768,0,0,0,0] and g=[0.0138, 0.0414, -0.0525, -0.2679, 0.0718, 0.9667, -0.9667, -0.0718, 0.2679, 0.0525, -0.0414, -0.0138] [38], respectively, and 5 level decomposition is used. Then the WTF and WETF can be calculated using the formula (7) and (16), respectively. Finally, the following comparisons are made.

- **Relationship with TF**: With the 5 level decomposition, the wavelet transform (WT) of each measurement produce 6 groups of wavelet coefficients, namely, $D_1, D_2, D_3, D_4, D_5, A_5$ where D_1 group contains the highest frequency components and A_5 denotes the lowest frequency components and others represent middle frequencies. Further, the wavelet transforms are essentially the filters and therefore the wavelet coefficients are the filtered results of original signal followed by down sampling. In other words, the wavelet coefficients from each group can be regarded as the filtered time-series data. Different from the TF plot that shows the frequency response, both WTF and WETF plots as shown in Figs. 5 and Fig. 6 can be classified into six different groups where each contains multiple frequency components. Further, within each group, both of WTF and WETF have repeatable patterns under noise-free conditions and time-invariant loadings. More importantly, WETF has a high ratio in the lowest frequency group represented by $E(A_5^2/A_5^1)$ and lower ratios in other higher frequency groups, which shares the similar trends. This is because the wavelet energy ratio can be interpreted as an average of the mean squared TF frequency gains, which is proved as follows. Suppose $\mathbf{V}_1 = [\nu_1((z-1)m+1), ..., \nu_1(zm)]$ and $\mathbf{V}_2 = [\nu_2((z-1)m+1), ..., \nu_2(zm)]$ are wavelet transforms of the two measurements and they belong to the defined wavelet energy group $z, z = 1, ..., Z$. Since the wavelet coefficients from each level decomposition can be interpreted as the filtered measurement data and the frequency components in a bounded frequency range, $\mathbf{V}_1$ used in the zth group of WETF can be written in a Fourier Series form, i.e.

$$\nu_1(h) = \sum_{k=lf}^{sf} x_k e^{-i2\pi kh} \tag{22}$$

where lf and sf represent the lower bound and upper bound frequency components, respectively, and $h = (z-1)m+1, \ldots, zm$. Since $\nu_2(h)$ can be treated as the output of TF under the input of $\nu_1(h)$, it can be written as

$$\nu_2(h) = \sum_{k=lf}^{sf} c_k x_k e^{-i2\pi kh} \tag{23}$$

where c_k is the gain at the frequency k. By using Parseval's theorem [39], the proposed WETF given by (16) with two measurements can be re-written as

$$\begin{aligned} t(z) = \frac{e_2(z)}{e_1(z)} &= \sqrt{\frac{\sum_{h=(z-1)m+1}^{zm} \nu_2^2(h)}{\sum_{h=(z-1)m+1}^{zm} \nu_1^2(h)}} \\ &= \sqrt{\frac{\sum_{k=lf}^{sf} c_k^2 x_k^2}{\sum_{k=lf}^{sf} x_k^2}} \end{aligned} \tag{24}$$

As $t(z)$ is in a limited frequency range and bounded within $[lf, sf]$, all the gains c_k's are similar and it is reasonable to suppose all the gains can be approximated using a single value $c \in [c_{min}, c_{max}]$ where c_{min} and c_{max} represent the minimal and maximal gains within the frequency range $[lf, sf]$, respectively. And then the formula (24) can be simplified to

$$\begin{aligned} t(z) = \frac{e_2(z)}{e_1(z)} &= \sqrt{\frac{\sum_{k=lf}^{sf} c_k^2 x_k^2}{\sum_{k=lf}^{sf} x_k^2}} \\ &= \sqrt{\frac{\sum_{k=lf}^{sf} c^2 x_k^2}{\sum_{k=lf}^{sf} x_k^2}} \\ &= c \end{aligned} \tag{25}$$

This indicates that the proposed WETF can be interpreted as a gain of TF within the corresponding frequency range. In other words, the proposed WETF has a clear physical meaning.

- **Robustness to noise**: The noise with 20 dB signal-to-noise (SNR) ratio is added to the first measurement. The noisy first measurement passes through the TF and this results in the noisy second measurement. Both the WTF and the WETF under the noisy condition are plotted in Figs. 7 and Fig. 8, respectively. Compared to noise-free case, the WTF is significantly changed with noise, particularly, repeatable patterns are corrupted. However, the WETF keeps the same trends as those in the noise free case. In other words, the WTF is very sensitive to noise but the WETF is robust to noise.
- **Robustness to time-varying loading**: For a non-stationary process, varying loading has a directly impact on each measurement. Here, suppose the loading only changes once at the half time and therefore two loading conditions are produced. The first half measurement is under one loading as mentioned above and the latter is under another loading, say a doubled amplitude loading. Results from Figs. 9 and 10 show that varying loading can change the WTF but it has negligible impact on the WETF. Therefore, the WETF is insensitive to varying loading and can be used for non-stationary applications.
- **Sensitivity to system property change**: To test the sensitivity of both WTF and WETF under the condition of system property changes, the experiment is repeated but the system property is changed under the second loading condition. More specifically, the system under two loading conditions has two different TFs that are shown in Fig. 11 where the first one labeled 'tf1' is given by (21) and the second one labeled by 'tf2' is given by

$$TF(s) = \frac{36s + 900}{s^2 + 36s + 900} \tag{26}$$

The main differences between the two TFs lie in the low frequency gains. It is desirable to capture the system change under different loading conditions. It seems hard to capture the change from the WTF plot shown in Fig. 12. In contrast, it is easy to observe the change from the WETF plot in Fig. 13. WETF correctly indicates the change in the first group with low frequency range that is label using a rectangle. Further, as the results of wavelet transforms include time information, it can be seen from Fig. 13 that the change happens in the second half part,

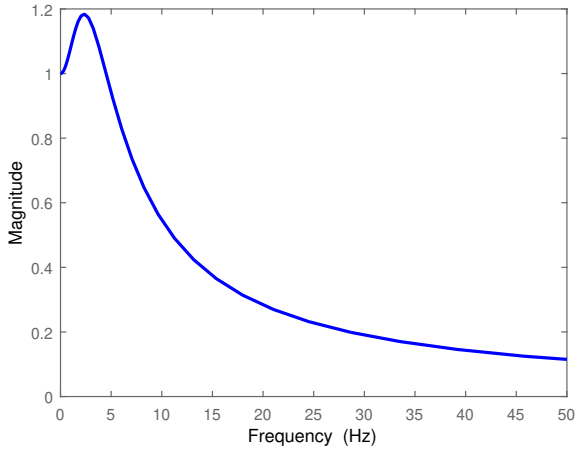

Fig. 4. Transmissibility function of the system used in the numerical example

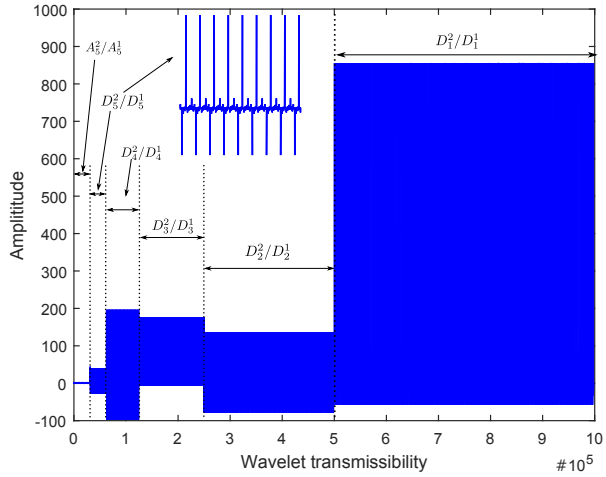

Fig. 5. Wavelet transmissibility function of the system used in the numerical example

which accurately captures the change due to the second loading.

In order to fully understand the WETF, some discussions are summarized as follows:

- **Group number determination**: It is important to know how to determine the total group number Z. Both time-varying loads and noise have an impact on the group number. More specifically, time-varying or non-stationary loads can be formulated as a combination of a number of time-invariant or stationary loads, say the number is Z_0 under the given sampling time. The basic requirement is that each group represents a full or part of stationary process. Therefore, the chosen group number Z should be bigger than Z_0, e.g. $Z > Z_0$. Further, each group should include sufficient data points where the noise, generally Gaussian noise, can have minimal impact on each group, and then the RMS values would be consistent. On the other hand, the sufficient data in each group requires that group number should not be bigger than an upper bound value, say Z_1. In some cases, Z_0 could be known. For example, wind is time varying but statistical study

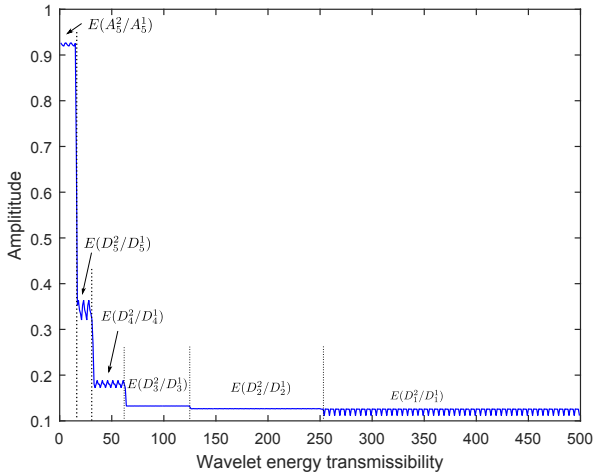

Fig. 6. Wavelet energy transmissibility function of the system used in the numerical example

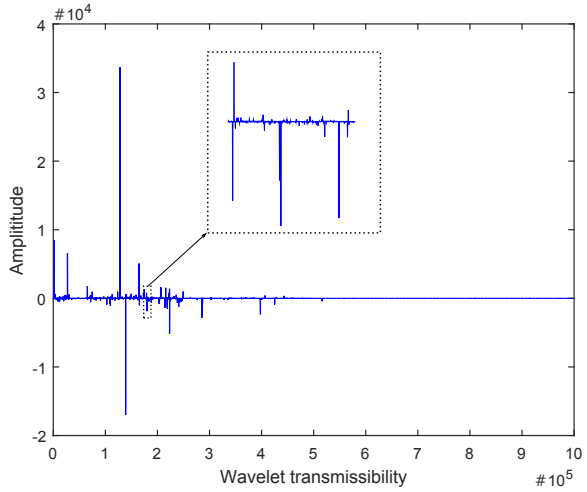

Fig. 7. Wavelet transmissibility function of the system used in the numerical example under noise with 20 SNR

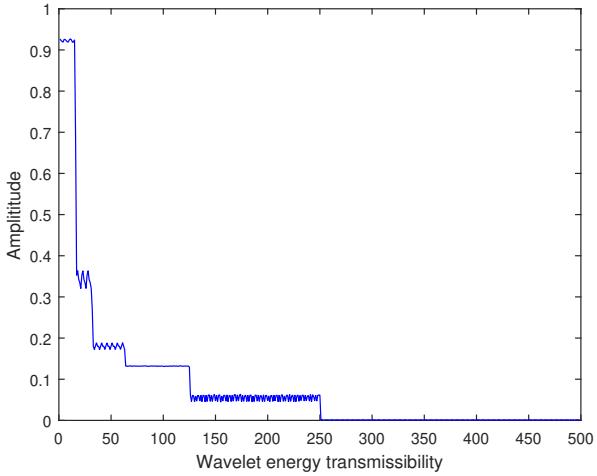

Fig. 8. Wavelet energy transmissibility function of the system used in the numerical example under noise with 20 SNR

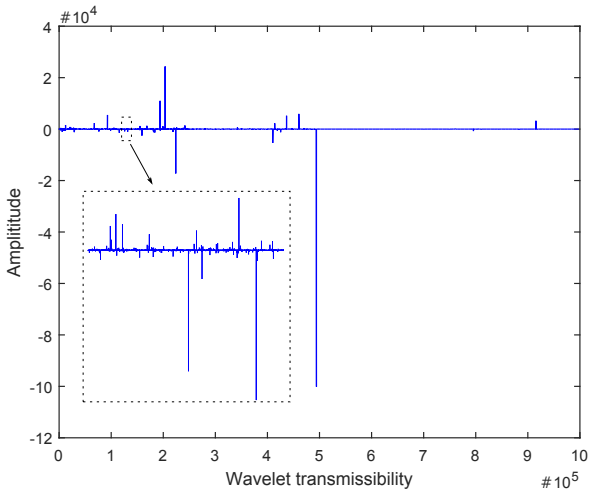

Fig. 9. Wavelet transmissibility function of the system used in the numerical example under varying loading conditions

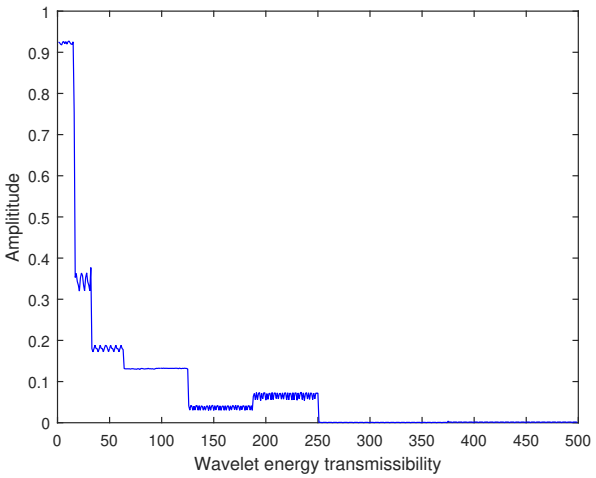

Fig. 10. Wavelet energy transmissibility function of the system used in the numerical example under varying loading conditions

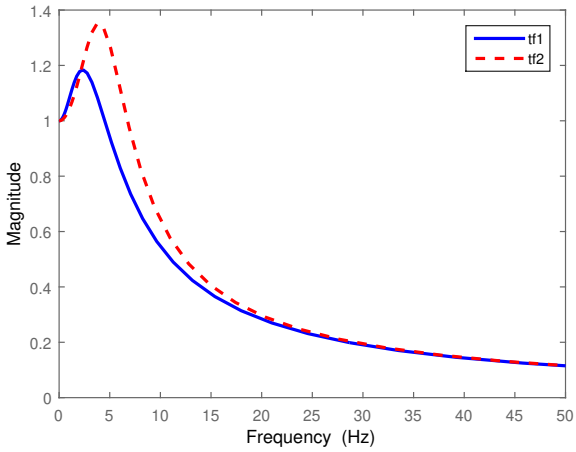

Fig. 11. Two transmissibility functions of the system used in the numerical example

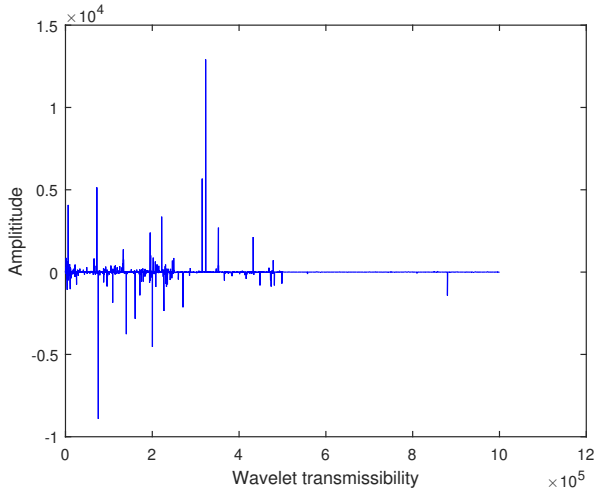

Fig. 12. Wavelet transmissibility function of the system with property change used in the numerical example

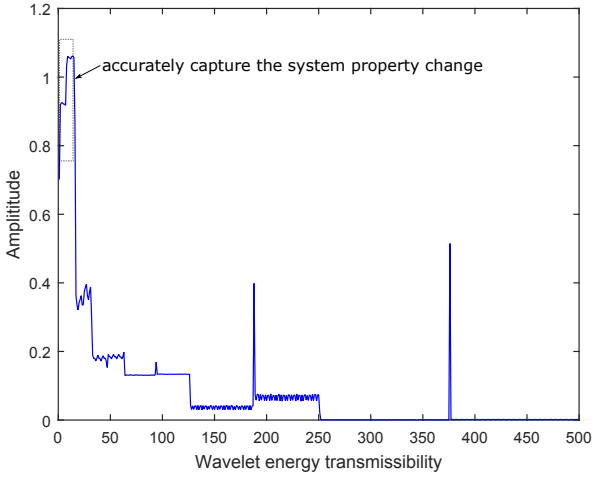

Fig. 13. Wavelet energy transmissibility function of the system with property change used in the numerical example

shows it can be treated a stationary process in a short time of 10 seconds. If the measurement sampling time lasts for 100 seconds, then the total group number is at least 10 in order to make sure that each group represents a stationary process. In some practical cases, Z_0 and Z_1 may be unknown. Therefore, trials and errors can be used to choose the group number Z.

- **WTF is a special case of WETF**: When applying the WETF, if the group number is chosen as its maximal value, i.e. the length of the whole measured data and each group of WETF only has one data, it can be easily to observe that the WETF becomes the WTF. Therefore, the WTF is a special case of the WETF. The WTF has only one single data in each group. This means that it has extremely insufficient data in each group, which results in the high sensitivity to noise. This conclusion is also confirmed using both numerical examples in the current section and the real world case study in the following section.

- **Reference**: In practice, if no healthy condition reference is available, the proposed method can still be used. The current state, even with some defects, can be used as the reference and further deterioration causing more severe defects can be shown in the TDI values.
- **Incipient fault detection and prognosis**. It is very important to detect the incipient faults at an early stage. However, conventional spectral methods often fail to do so under the time-varying loading conditions. The reason for this is that the time-varying loading can lead to varying spectra. The incipient faults with slight changes in the spectra may not be identifiable. The proposed methods can effectively deal with the varying loading impact and therefore it can be used for incipient fault detection. The TDI indicators using the WETF can be used for inferring both damage and severity level detection. Further, the trending of TDI indicators can be used for prognosis to predict the future deterioration rate and even failure time by using some curve analysis methods. It is worth pointing out that, to monitor the incipient faults, data collection should last for a long enough periods, sometimes several years, including both healthy condition and changed conditions. If the proposed method is applied for the continuously monitored data, TDI indicator values will be reduced, often slowly drifted due to the low change in the condition, which can be used to distinguish the incipient damage from the healthy condition because the used TDI indicator is a quantitative evaluation of differences between the reference and in-serve condition.
- **Differences from existing wavelet methods**: First, the unique contribution of this paper is that the novel method does not require or measure loading information but it is able to remove the impact of varying loadings for non-stationary applications. Some popular methods reported in [40] have to measure and use information such as rotation speed in order to deal with time varying conditions. Further, the proposed method is computationally efficient as its main computation is from wavelet decomposition and it does not require a complex training process. A number of existing methods which are a combination of the extracted wavelet features and artificial intelligent algorithms [41], [42], require a large amount training data and a complex training process.
- **Advantages and limitations**: The main advantage is that the new WETF is related to system physical properties and therefore can present the system conditions. Further, the WETF is able to deal with multiple system responses without requiring the system input. Finally, the WETF is computationally efficient as it only needs calculating wavelet decomposition and RMS. The main limitation, as pointed in [27], [43], is that the values of TF depend on location of system input. In this case, multiple WETFs under inputs at different locations can be used to address the varying position problem [34], which will be investigated in future studies.

In this section, the novel concept, WETF, has been introduced and its robustness to dynamic loading and noise has been analyzed in theory and also validated using a numerical example. The application of the novel method to the real-world problem will be investigated in the following section.

IV. Wind Turbine Bearing Condition Monitoring

Worldwide installed wind turbines have been significantly increased over the past decade. To avoid unexpected failure and minimize turbine downtime, different wind turbine condition monitoring systems and methods have been developed [44], [45], [46], [47], [48]. Although a number of methods have been proposed, most of them are tested in simulation or lab stage and have not been fully tested in operating wind turbines [3]. In this section, the real world wind turbine condition monitoring problem is considered. Two condition monitoring systems were installed on two operating turbines in Greece, which were carried out by an industrial partner in a joint project funded by European Research Council. The vibration data from four acceleration sensors fitted on the main bearing were collected. It is known that one bearing was in good conditions while the other had some damaging conditions over the period of monitoring. It has to mention that for the purpose of condition monitoring, data collection should last for a long enough period including both healthy condition and changed conditions. However, often in practice, no reference data were recorded during the healthy condition. To deal with this issue, an alternative option is to use the healthy data from another system that has the same physical structures but is in good condition. A number of examples in the literature also used another system as a reference [9], [49], [10], [50], [13], [21]. The four acceleration type vibration sensors were fitted at different locations along the main bearing. The employed sampling rate was 25 KHz and each data collection lasted for 12 seconds, producing 300000 data points from each sensor. The data acquisition was carried out hourly and had a duration of about 5 months.

In order to show the time-varying loading effects, four data sets that were collected at different time under good conditions were plotted in Fig. 14, where the data collection date was labeled below each sub-figure, e.g. 20140324 representing 24th March 2014. It can be seen that the four sub-figures have different amplitudes ranges, indicating different loading conditions. Similar phenomena can be observed in Fig. 15 where the data were collected under damaging conditions. Further, the wavelet transforms (WT) of good condition and damaging condition data collected at different times are plotted in Fig. 16 and Fig. 17, respectively, where the low pass filter in (5) and high pass filter in (4) are chosen as h=[0,0,0,0,0.1768,0.5303,0.5303,0.1768,0,0,0,0] and g=[0.0138, 0.0414, -0.0525, -0.2679, 0.0718, 0.9667, -0.9667, -0.0718, 0.2679, 0.0525, -0.0414, -0.0138] [38], respectively. It can be seen that the wavelet coefficients varies from one sub-figure to another, which also shows the time-varying loading effects. However, the differences between good and bad conditions can not be observed from the wavelet coefficients due to their variations. Finally, the WTFs under good and damaging conditions are shown in Fig. 18 and Fig.

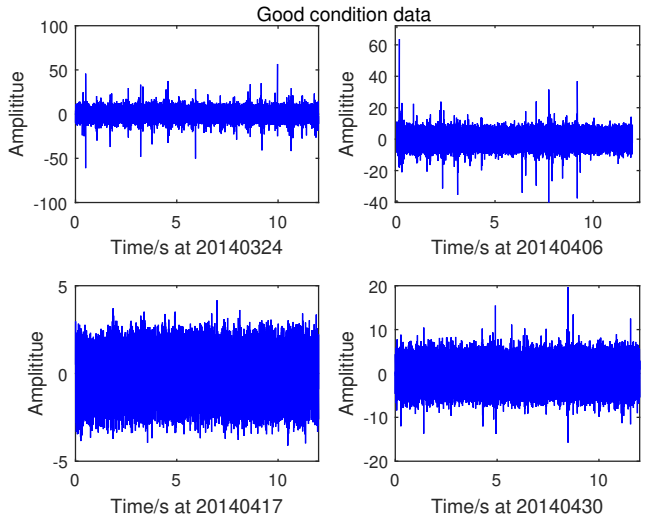

Fig. 14. Time series vibration data of good condition collected at different times

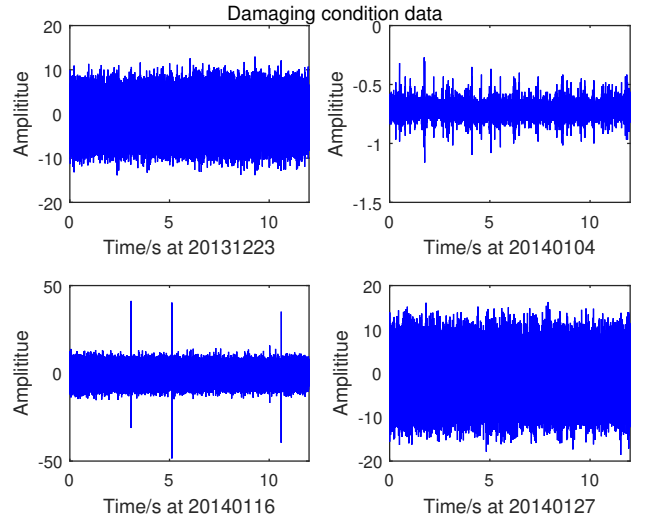

Fig. 15. Time series vibration data of damaging condition collected at different times

19, respectively. It is obviously still hard to tell the differences between good and damaging condition from the WTF due to the variations. Further, the TDI results using WTF are shown in Fig. 20, showing that the good condition has some difference compared with the bad conditions. However, the differences between two conditions are very insignificant. TDI values for the first 2190 sets of good condition data are around 0.3. As the TDI values are in the range of [0,1], we need to choose a threshold to determine its condition. Here, if we choose 0.5 as the threshold value, the good condition can be easily misinterpreted as bad conditions due to the small TDI values.

The new WETF is then used to analyze the same data sets. The grouped wavelet coefficients of good and damaging condition data collected at different times is plotted in Fig. 21 and Fig. 22, respectively, where the number of wavelet m in each group is chosen as 30 by trial-and-error. It is worth

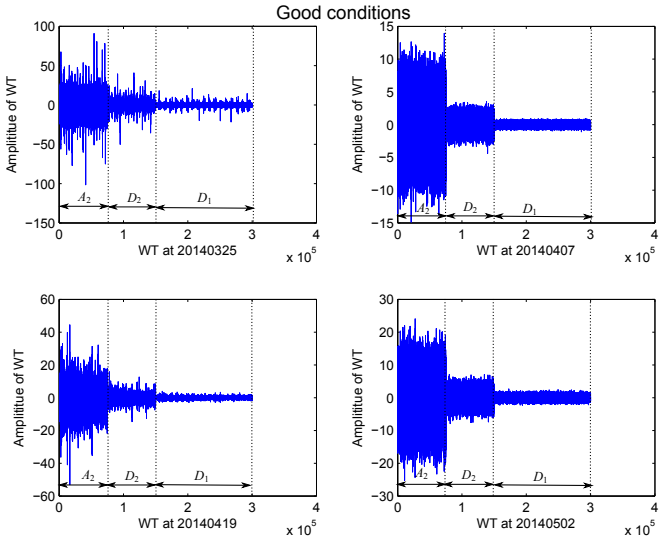

Fig. 16. WT of good condition data collected at different times

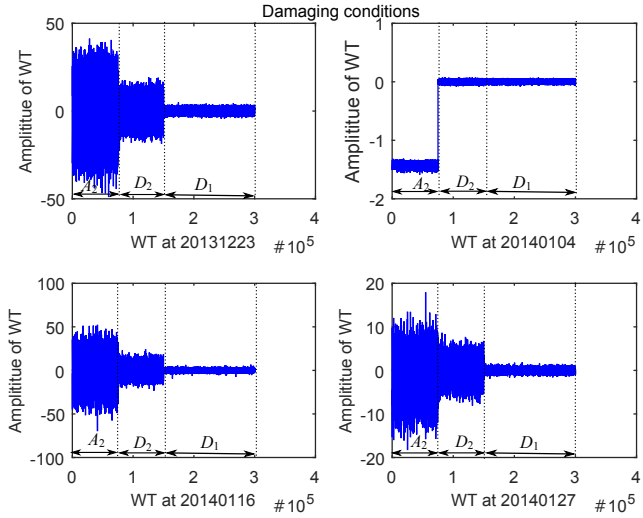

Fig. 17. WT of bad condition data collected at different times

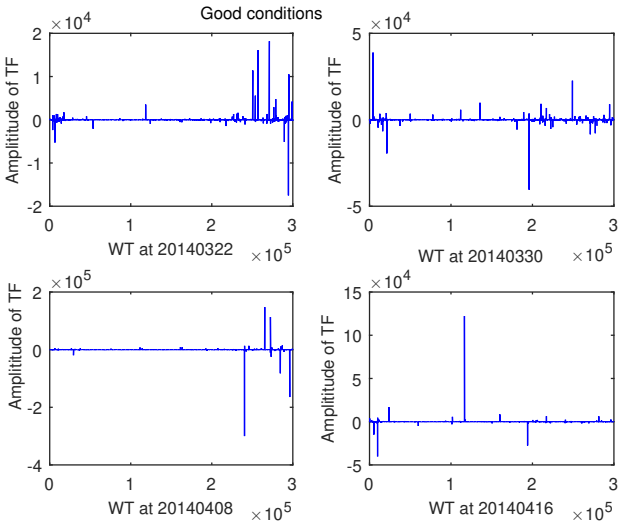

Fig. 18. WTFs of good condition data collected at different times

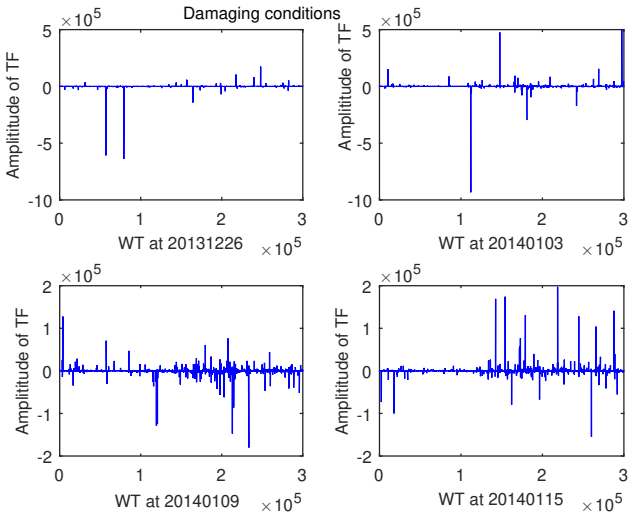

Fig. 19. WTFs of bad condition data collected at different times

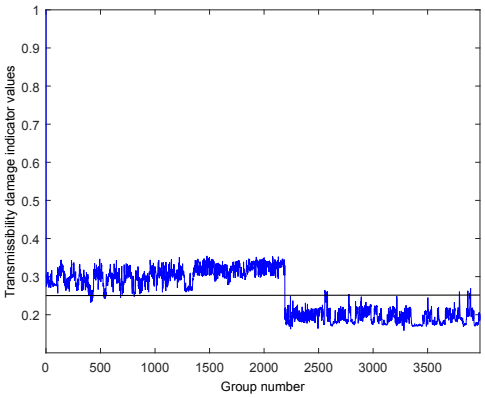

Fig. 20. TDI results using WTF method where data sets (1-2190 datasets: good condition, 2191-3990 datasets: damaging condition)

pointing out that the choice of m for other applications should follow the suggestion given in Section III. It can be seen that the amplitudes of grouped wavelet coefficients varies from one sub-figure to another sub-figure, still indicating different loading conditions on different data collection. Further, the WETF under good and damaging conditions are shown in Fig. 23 and Fig. 24, indicating the WETFs with good condition under different loading conditions are quite similar. In other words, the WETF is robust to variable loadings and noise. Therefore, it can be used as a good indicator of true system condition. The same conclusion can also be observed from WETFs for the data under damaging condition at different loading conditions. Finally, TDI result using WETF is given in Fig. 25. Compared to the previous results produced by WTF shown in Fig. 20, the new results shown in Fig. 25 can clearly distinguish the differences between good and damaging conditions without a false alarm if choosing 0.5 as the threshold. To make a fair comparison, the threshold for the conventional WTF method has been chosen as 0.25 as all its TDI values as shown in Fig. 20 are smaller than those for the proposed method. It is found that there are 85 false alarms for

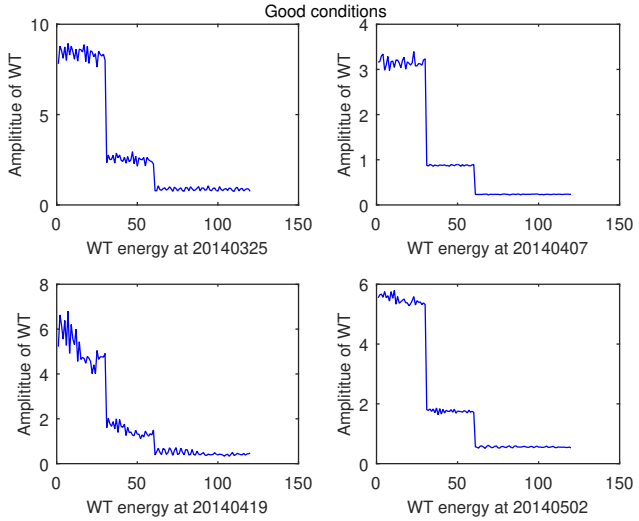

Fig. 21. The RMS values of the grouped WT coefficients of good condition data collected at different times

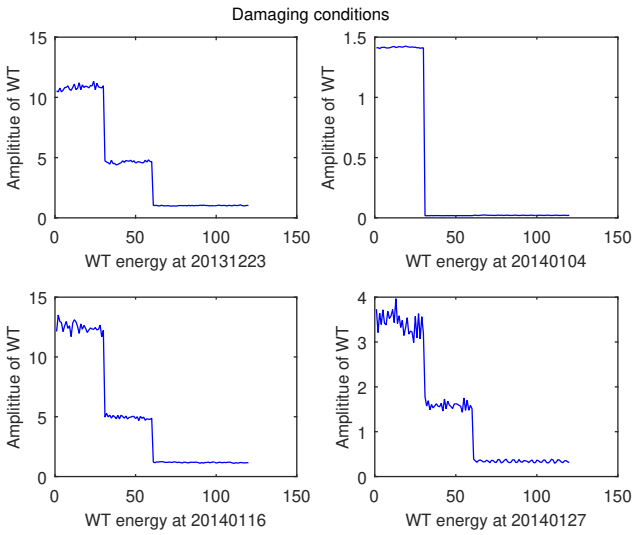

Fig. 22. The RMS values of the grouped WT coefficients of bad condition data collected at different times

the WTF method. This comparison confirms the advantages of the new WETF approach over the WTF method.

V. Conclusion

In this paper, a new wavelet energy transmissibility analysis method is proposed and has been applied to field data from operating wind turbines for wind turbine bearing condition monitoring. The main advantage of the WETF is that it can be used for condition monitoring under non-stationary operations and the result is insensitive to time-varying loads and noise. The results of the analysis using the field data have shown the new method can produce much better indicator than the direct wavelet transmissibility analysis for evaluating the conditions of wind turbine bearings.

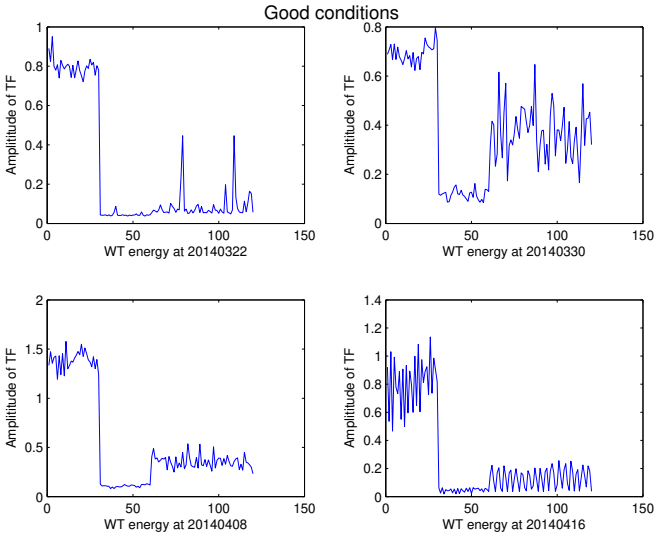

Fig. 23. WETF of good condition data collected at different times

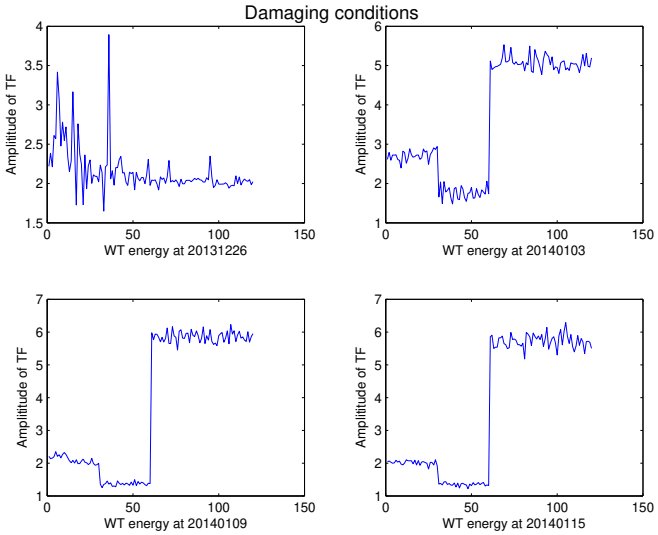

Fig. 24. WETF of bad condition data collected at different times

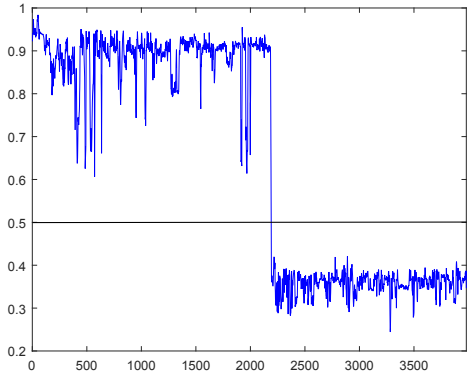

Fig. 25. TDI results using the proposed WETF method (1-2190 datasets: good condition, 2191-3990 datasets: damaging condition)

ACKNOWLEDGEMENT

The authors would like to thank D2S international (http://www.d2sint.com/) for kindly providing the field data.

REFERENCES

[1] F. P. G. Márquez, A. M. Tobias, J. M. P. Pérez, and M. Papaelias, "Condition monitoring of wind turbines: techniques and methods," *Renewable Energy*, vol. 46, pp. 169–178, 2012.

[2] W. Qiao and D. Lu, "A survey on wind turbine condition monitoring and fault diagnosis-part ii: Signals and signal processing methods," *IEEE Transactions on Industrial Electronics*, vol. 62, no. 10, pp. 6546 – 6557, 2015.

[3] W. X. Yang, P. J. Tavner, C. J. Crabtree, Y. Feng, and Y. Qiu, "Wind turbine condition monitoring: technical and commercial challenges," *Wind Energy*, vol. 17, no. 5, pp. 673–693, 2014.

[4] B. Lu, Y. Li, X. Wu, and Z. Yang, "A review of recent advances in wind turbine condition monitoring and fault diagnosis," in *IEEE Power Electronics and Machines in Wind Applications (PEMWA), 2009.* IEEE, 2009, pp. 1–7.

[5] W. Bartelmus and R. Zimroz, "A new feature for monitoring the condition of gearboxes in non-stationary operating conditions," *Mechanical Systems and Signal Processing*, vol. 23, no. 5, pp. 1528–1534, 2009.

[6] S. Cruz, "An active-reactive power method for the diagnosis of rotor faults in three-phase induction motors operating under time-varying load conditions," *IEEE Transactions on Energy Conversion*, vol. 27, no. 1, pp. 71–84, 2012.

[7] R. R. Schoen and T. G. Habetler, "Evaluation and implementation of a system to eliminate arbitrary load effects in current-based monitoring of induction machines," vol. 33, no. 6, pp. 1571–1577, 1997.

[8] R. Zimroz, W. Bartelmus, T. Barszcz, and J. Urbanek, "Diagnostics of bearings in presence of strong operating conditions non-stationarity a procedure of load-dependent features processing with application to wind turbine bearings," *Mechanical Systems and Signal Processing*, vol. 46, no. 1, pp. 16–27, 2014.

[9] W. Bartelmus and R. Zimroz, "Vibration condition monitoring of planetary gearbox under varying external load," *Mechanical Systems and Signal Processing*, vol. 23, no. 1, pp. 246–257, 2009.

[10] W. Bartelmus, F. Chaari, R. Zimroz, and M. Haddar, "Modelling of gearbox dynamics under time-varying nonstationary load for distributed fault detection and diagnosis," *European Journal of Mechanics-A/Solids*, vol. 29, no. 4, pp. 637–646, 2010.

[11] I. Antoniadou, G. Manson, W. J. Staszewski, T. Barszcz, and K. Worden, "A time–frequency analysis approach for condition monitoring of a wind turbine gearbox under varying load conditions," *Mechanical Systems and Signal Processing*, vol. 64-65, pp. 188–216, 2015.

[12] X. Y. Wang, V. Makis, and M. Yang, "A wavelet approach to fault diagnosis of a gearbox under varying load conditions," *Journal of Sound and Vibration*, vol. 329, no. 9, pp. 1570–1585, 2010.

[13] R. B. Randall and J. Antoni, "Rolling element bearing diagnostics a tutorial," *Mechanical Systems and Signal Processing*, vol. 25, no. 2, pp. 485–520, 2011.

[14] E. S. Carbajo, R. S. Carbajo, C. McGoldrick, and B. Basu, "Asdah: An automated structural change detection algorithm based on the hilbert–huang transform," *Mechanical Systems and Signal Processing*, vol. 47, no. 1, pp. 78–93, 2014.

[15] S. Nagarajaiah and B. Basu, "Output only modal identification and structural damage detection using time frequency & wavelet techniques," *Earthquake Engineering and Engineering Vibration*, vol. 8, no. 4, pp. 583–605, 2009.

[16] B. Basu, S. Nagarajaiah, and A. Chakraborty, "Online identification of linear time-varying stiffness of structural systems by wavelet analysis," *Structural Health Monitoring*, vol. 7, no. 1, pp. 21–36, 2008.

[17] D. Cantero and B. Basu, "Railway infrastructure damage detection using wavelet transformed acceleration response of traversing vehicle," *Structural Control and Health Monitoring*, vol. 22, no. 1, pp. 62–70, 2015.

[18] J. Abe, Ma.and Abot and B. Basu, "Encyclopedia of structural health monitoring."

[19] H. Zoubek, S. Villwock, and M. Pacas, "Frequency response analysis for rolling-bearing damage diagnosis," *IEEE Transactions on Industrial Electronics*, vol. 55, no. 12, pp. 4270–4276, 2008.

[20] L. Gelman, "The new frequency response functions for structural health monitoring," *Engineering Structures*, vol. 32, no. 12, pp. 3994–3999, 2010.

[21] L. Zhang, Z. Q. Lang, and M. Papaelias, "Generalized transmissibility damage indicator with application to wind turbine component condition monitoring," *IEEE Transactions on Industrial Electronics*, vol. 63, no. 10, pp. 6347–6359, 2016.

[22] S. N. Ganeriwala, J. Yang, and M. Richardson, "Using modal analysis for detecting cracks in wind turbine blades," *Sound and Vibration*, vol. 45, no. 5, p. 10, 2011.

[23] A. M. R. Ribeiro, J. M. M. Silva, and N. M. M. Maia, "On the generalisation of the transmissibility concept," *Mechanical Systems and Signal Processing*, vol. 14, no. 1, pp. 29–35, 2000.

[24] M. J. Schulz, A. S. Naser, P. F. Pai, M. S. Linville, and J. Chung, "Detecting structural damage using transmittance functions," in *Proceddings SPIE the Intertional Society for Optical Engineering*. SPIE the International Society for OpticalL, 1997, pp. 638–644.

[25] T. J. Johnson and D. E. Adams, "Transmissibility as a differential indicator of structural damage," *Journal of Vibration and Acoustics*, vol. 124, no. 4, pp. 634–641, 2002.

[26] T. J. Johnson, R. L. Brown, D. E. Adams, and M. Schiefer, "Distributed structural health monitoring with a smart sensor array," *Mechanical Systems and Signal Processing*, vol. 18, no. 3, pp. 555–572, 2004.

[27] S. Chesné and A. Deraemaeker, "Damage localization using transmissibility functions: a critical review," *Mechanical systems and signal processing*, vol. 38, no. 2, pp. 569–584, 2013.

[28] K. Worden, G. Manson, and D. Allman, "Experimental validation of a structural health monitoring methodology: Part i. novelty detection on a laboratory structure," *Journal of Sound and Vibration*, vol. 259, no. 2, pp. 323–343, 2003.

[29] W. X. Yang, Z. Q. Lang, and W. Y. Tian, "Condition monitoring and damage location of wind turbine blades by frequency response transmissibility analysis," *IEEE Transactions on Industrial Electronics*, vol. 62, no. 10, pp. 6558–6564, 2015.

[30] W. J. Staszewski and D. M. Wallace, "Wavelet-based frequency response function for time-variant systems - an exploratory study," *Mechanical Systems and Signal Processing*, vol. 47, no. 1, pp. 35–49, 2014.

[31] K. Dziedziech, W. J. Staszewski, B. Basu, and T. Uhl, "Wavelet-based detection of abrupt changes in natural frequencies of time-variant systems," *Mechanical Systems and Signal Processing*, vol. 64, pp. 347–359, 2015.

[32] B. Basu, "Identification of stiffness degradation in structures using wavelet analysis," *Construction and building materials*, vol. 19, no. 9, pp. 713–721, 2005.

[33] S. G. Mallat, "A theory for multiresolution signal decomposition: the wavelet representation," *IEEE Transactions on Pattern Analysis and Machine Intelligence*, vol. 11, no. 7, pp. 674–693, 1989.

[34] N. M. M. Maia, R. A. B. Almeida, A. P. V. Urgueira, and R. P. C. Sampaio, "Damage detection and quantification using transmissibility," *Mechanical Systems and Signal Processing*, vol. 25, no. 7, pp. 2475–2483, 2011.

[35] L. Zhang, Z. Q. Lang, and W. X. Yang, "Wavelet transmissibility analysis for wind turbine blade condition monitoring," in *2015 International Conference on Condition Monitoring and Machinery Failure*, 2015, pp. 1–4.

[36] Z. Q. Yang, "Wavelet transmissibility analysis for wind turbine condition monitoring," Master's thesis, Univerity of Manchester, 2016.

[37] Y. E. Lage, M. M. Neves, N. M. M. Maia, and D. Tcherniak, "Force transmissibility versus displacement transmissibility," *Journal of Sound and Vibration*, vol. 333, no. 22, pp. 5708–5722, 2014.

[38] S. Mallat, *A wavelet tour of signal processing*. Academic press, 1999.

[39] D. G. Manolakis and V. K. Ingle, *Applied digital signal processing: theory and practice*. Cambridge University Press, 2011.

[40] H. H. Bafroui and A. Ohadi, "Application of wavelet energy and shannon entropy for feature extraction in gearbox fault detection under varying speed conditions," *Neurocomputing*, vol. 133, pp. 437–445, 2014.

[41] A. A. Yusuff, C. Fei, A. A. Jimoh, and J. L. Munda, "Fault location in a series compensated transmission line based on wavelet packet decomposition and support vector regression," *Electric Power Systems Research*, vol. 81, no. 7, pp. 1258–1265, 2011.

[42] M. A. Jafarizadeh, R. Hassannejad, M. M. Ettefagh, and S. Chitsaz, "Asynchronous input gear damage diagnosis using time averaging and wavelet filtering," *Mechanical Systems and Signal Processing*, vol. 22, no. 1, pp. 172–201, 2008.

[43] D. Christof, P. Flavio, D. S. Gert, V. Katy, D. T. Troyer, S. Vanlanduit, and P. Guillaume, "Structural health monitoring in changing operational conditions using tranmissibility measurements," *Shock and Vibration*, vol. 17, no. 4-5, pp. 651–675, 2010.

[44] L. Stankovic, V.and Stankovic, S. Wang, and S. Cheng, "Distributed compression for condition monitoring of wind farms," *IEEE Transactions on Sustainable Energy*, vol. 4, no. 1, pp. 174–181, 2013.

[45] P. Guo, D. Infield, and X. Yang, "Wind turbine generator condition-monitoring using temperature trend analysis," *IEEE Transactions on sustainable energy*, vol. 3, no. 1, pp. 124–133, 2012.

[46] A. Kusiak and A. Verma, "A data-driven approach for monitoring blade pitch faults in wind turbines," *IEEE Transactions on Sustainable Energy*, vol. 2, no. 1, pp. 87–96, 2011.

[47] F. Cheng, L. Qu, and W. Qiao, "Fault prognosis and remaining useful life prediction of wind turbine gearboxes using current signal analysis," *IEEE Transactions on Sustainable Energy*, 2017.

[48] S. Shokrzadeh, M. J. Jozani, and E. Bibeau, "Wind turbine power curve modeling using advanced parametric and nonparametric methods," *IEEE Transactions on Sustainable Energy*, vol. 5, no. 4, pp. 1262–1269, 2014.

[49] W. Bartelmus and R. Zimroz, "A new feature for monitoring the condition of gearboxes in non-stationary operating conditions," *Mechanical Systems and Signal Processing*, vol. 23, no. 5, pp. 1528–1534, 2009.

[50] G. K. Chaturvedi and D. W. Thomas, "Bearing fault detection using adaptive noise cancelling," *Journal of Mechanical Design*, vol. 104, no. 2, pp. 280–289, 1982.